Available online at www.sciencedirect.com
ScienceDirect
Trans. Nonferrous Met. Soc. China 25(2015) 2230−2240
Transactions of Nonferrous Metals Society of China
www.tnmsc.cn

Sintering preparation of porous sound-absorbing materials from steel slag

Peng SUN, Zhan-cheng GUO

State Key Laboratory of Advanced Metallurgy, University of Science and Technology Beijing, Beijing 100083, China

Received 22 September 2014; accepted 28 December 2014

Abstract: Porous sound-absorbing materials were prepared from steel slag using waste expanded polystyrene (EPS) particles as pore former. The influences of the experimental conditions such as fly ash content, sintering temperature, sintering time, and pore former addition on the performance of the porous sound-absorbing materials were investigated. The results show that the porosity of the specimens can reach above 50.0%; the compressive strength and average sound-adsorption coefficient of the sintered specimens are above 3.0 MPa and 0.47, respectively. The optimum preparation conditions for the steel slag porous sound-absorbing materials are as follows: mass fraction of fly ash 50%, waste EPS particles 3.6 g, sintering temperature 1100 °C, and sintering time 7.5 h, which are determined by considering the properties of the sound-absorbing materials, energy consumption and cost.

Key words: steel slag; porous sound-absorbing material; noise reduction coefficient; porosity; compressive strength

1 Introduction

Steel slag is a by-product of steel production that makes up about 15% of steel output [1]. The utilization ratio of steel slag in China is less than 22%, and around 60 million additional tons of steel slags are discharged per year. The steel slag dumps occupy large areas of land and result in many serious environmental problems. Therefore, it is of great concern to explore new, efficient ways of using steel slag in order to improve the utilization rateo.

The main chemical compositions of steel slag include calcium oxide (CaO), silicon dioxide (SiO_2), aluminium oxide (Al_2O_3), iron sesquioxide (Fe_2O_3), magnesium oxide (MgO), etc. The common minerals in steel slag are dicalcium silicate (C_2S), tri-calcium silicate (C_3S), dicalcium ferrite (C_2F), RO phase (CaO−FeO–MnO–MgO solid solution), and free CaO [2−7]. Because the steel slag has a high silicate composition, steel slag not only has certain cementitious properties, making it useful as an admixture for cement and concrete [8−13], but it also meets the chemical composition requirements for the preparation of glass–ceramic and ceramics. It can thus be used for preparing slag glass ceramics, ceramics, and other materials [14−17]. As the content of CaO in steel slag is high, generally between 40% and 60%, the siliceous materials need to be added to improve the cementitious properties, stability, sintering properties of steel slag used in building materials [18,19]. Fly ash contains a significant amount of SiO_2, Al_2O_3, Fe_2O_3 and other acidic oxides, a small amount of CaO, and so on. The first three oxides account for more than 75% of fly ash content [20−22]. Consequently, fly ash can be used as siliceous material in the preparation of structural materials by steel slag.

Noise pollution is becoming much severer issues. The use of porous sound absorption material is an important measure to control noise pollution. A sound wave is absorbed when the wave is transmitted into thermal energy, which then disperses into the air, by viscosity resistance, compression-expansion, and/or vibration-transmission of the sound wave through porous sound absorption materials [23]. Therefore, porous sound absorption materials must keep appropriate open porosity and have a lot of fine, uniform, and connected pores [24]. According to the substance, porous sound absorption materials are divided into three categories: organic polymer porous materials, porous metallic materials and inorganic porous materials. Most organic porous materials cannot endure high temperature and the porous metallic materials have a higher cost, while typical inorganic materials are fragile and hazardous to health [25]. New types of inorganic porous materials,

Foundation item: Project (2011AA06A105) supported by the National High-tech Research and Development Program of China
Corresponding author: Zhan-cheng GUO; Tel/Fax: +86-10-82375042; E-mail: zcguo@metall.ustb.edu.cn
DOI: 10.1016/S1003-6326(15)63865-1

such as porous ceramics and foam glass, have been paid more and more attention.

Some studies on the preparation of porous sound-absorbing material from industrial solid wastes such as fly ash, coal gangue, and blast furnace slag, have been done and show that the porous sound-absorbing materials have high porosity but poor mechanical property [26−28]. There are few studies on the preparation of porous sound absorption material by using steel slag besides our group. we have explored sintering preparation of porous sound absorption material [29] using steel slag particles with binder, and the porous sound-absorbing materials have large volume density, poor processing performance because of only particles packing and non-uniform sintering. In order to develop a new method of preparing porous sound absorption material by utilizing steel slag, we prepared porous sound-absorbing material from steel slag powder using fly ash [30,31], waste expanded polystyrene (EPS) particles, and sodium silicate as a modifier, pore former, and binder, respectively.

2 Experimental

2.1 Raw materials

Steel slag powder with a particle size of less than 0.074 mm was obtained from Laigang Group Taidong Industries Co., Ltd. (Laiwu, Shandong Province, China). Its chemical composition is listed in Table 1. Its mineralogical phases, which were determined by XRD analysis, are given in Fig. 1. The fly ash was low-calcium, grade II and its chemical composition is also shown in Table 1. The fly ash was supplied by Laigang Group Thermal Power Co., Ltd. (Laiwu, Shandong Province, China). The waste EPS particle size was between 1.0 and 2.0 mm and the EPS was laboratory-made. Sodium silicate with a modulus of 2.6−2.9 was obtained from Beijing Jingmian Tongda Trading Co., Ltd. (Fengtai District, Beijing, China). Sodium fluorosilicate, class AR, was purchased from Tianjin Guangfu Fine Chemical Research Institute (Xiqing District, Tianjin, China).

Table 1 Chemical compositions and contents of main materials

Material	Mass fraction/%						
	CaO	Fe_2O_3	SiO_2	Al_2O_3	MgO	MnO	P_2O_5
Steel slag	40.56	25.64	17.35	2.86	5.02	3.11	2.87
Fly ash	3.05	5.47	52.79	32.31	0.63	0.05	0.56

Material	Mass fraction/%						
	TiO_2	SO_3	V_2O_5	Cr_2O_3	K_2O	SrO	Na_2O
Steel slag	1.46	0.18	0.51	0.21	0.12	0.02	−
Fly ash	2.12	0.44	−	0.06	1.72	0.16	0.37

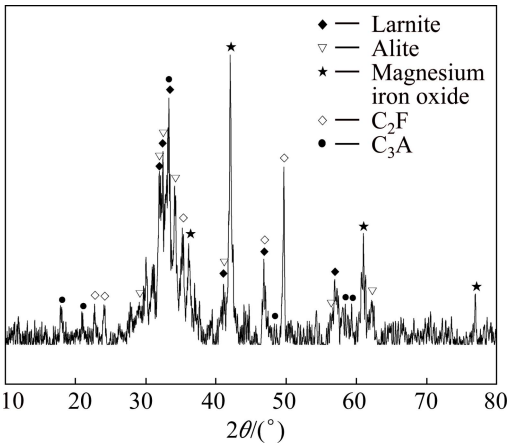

Fig. 1 XRD pattern of steel slag

2.2 Preparation of specimens

In accordance with the ratio of the raw materials, the steel slag and fly ash were weighed and mixed together. The mixed material was moistened with a little water for 30 min. The waste EPS was weighed and wetted using 10 mL of 5% sodium hydroxide solution. Then, the aged materials and waste EPS were mixed with 5% sodium silicate. The mixture was then molded. The rough blanks were demolded and dried for 48 h. According to the sintering procedure shown in Fig. 2, the rough blanks were put into a resistance furnace and sintered at 950, 1000, 1050, 1100, and 1150 °C for 4.5−9.0 h, respectively. Then, the steel slag sound-absorbing material samples with dimensions of (90−100) mm × 25 mm were prepared.

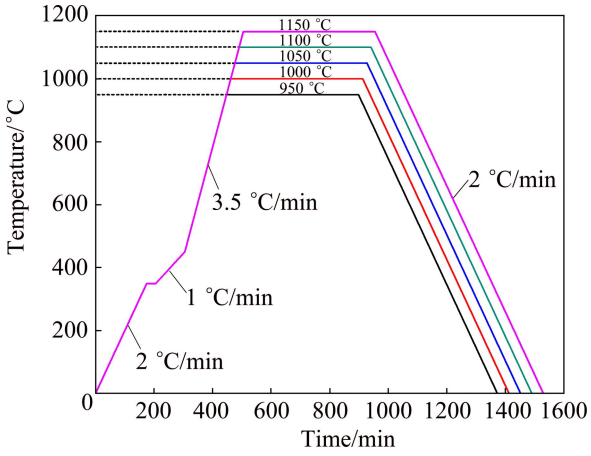

Fig. 2 Sintering procedure of steel slag sound-absorbing material

2.3 Characterization of specimens

The density and porosity of the specimens were determined by the Archimedes method, using deionized water as the immersion medium. Microstructural observation and pore distribution were performed using a mineral liberation analyzer (MLA−250). The main

mineral phases of the porous sound-absorbing material were measured by a powder X-ray diffractometer (XRD, DMAX-RB 12 kW, Rigaku) at a voltage of 40 kV and a current of 150 mA with Cu K_α radiation, and the detector scanned over a 2θ range of angles from 10° to 100° with a step size of 0.02°. The compressive strength of the specimen was measured by an MTS810 microcomputer control universal material testing machine with reference to test method for crushing strength of porous ceramic (GB/T 1964−1996). In accordance with Acoustics—Determination of sound absorption coefficient and impedance in impedance tubes—Part 1: Method using standing wave ratio, the sound-absorption properties of specimens of cylinders with diameters of 100 mm were tested by the standing-wave tube method, which is the normal incidence sound-absorbing determination.

3 Results and discussion

3.1 Effect of fly ash content on microstructure and properties of sound-absorbing material

The effect of the fly ash content on the structure and properties of the steel slag porous sound-absorbing material was investigated under the conditions of a sintering temperature of 1150 °C, a sintering time of 4.5 h, and 3.0 g of waste EPS. The density, porosity, and compressive strength of the specimens are presented in Table 2. With the increase of fly ash content, the density of the specimens increased from 1.37 to 1.59 g/cm^3, and the apparent porosity of the specimens was decreased by 5.4%. The compressive properties of the specimens were improved from 2.29 to 3.92 MPa.

Table 2 Effect of fly ash content on density, apparent porosity, and compressive strength of specimens

Mass fraction of fly ash/%	Density/ (g·cm^{-3})	Apparent porosity/%	Compressive strength/MPa
20	1.37	44.7	2.29
30	1.39	42.0	3.10
40	1.48	41.4	3.59
50	1.59	39.3	3.92

Figure 3 shows the morphology and distribution of the pores in the steel slag sound-absorbing material. The specimen with 30% fly ash (Fig. 3(a)) was relatively loose and had many more and larger pores. The specimen with 50% fly ash (Fig. 3(b)) was more compact, and had somewhat fewer and smaller pores. It was found from Figs. 3(c) and (d), which showed the micromorphology of the pores, that the addition of fly ash impacted the sintering of the base material under the same sintering conditions. The specimen with 30% fly ash had a more extensive crystal phase, with a visible crystal boundary

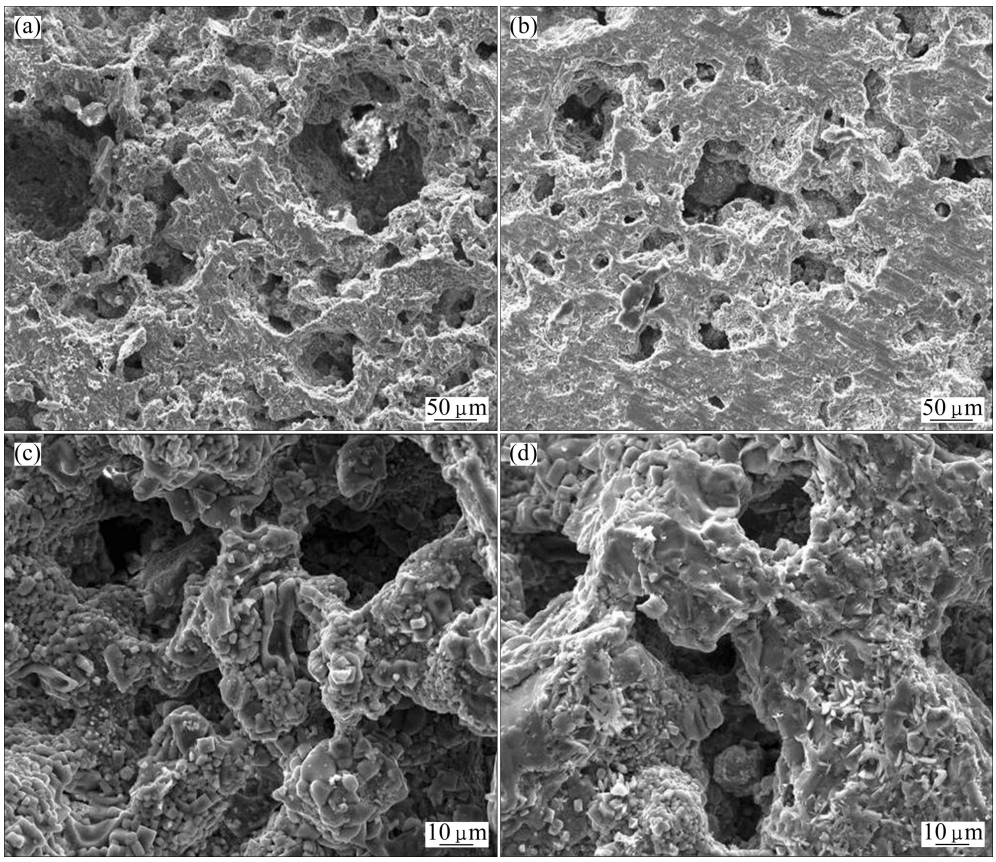

Fig. 3 SEM morphologies and distribution of pores in specimens with different fly ash contents: (a, c) 30% fly ash; (b, d) 50% fly ash

and crystals of different sizes and shapes. A pore network was formed and the sintering neck grew to a certain extent, but the specimen had a relatively low level of densification. For the specimen with 50% fly ash, the boundary of the crystal phase was not obvious and more glassy material was formed. The pore network was retained but the pore size decreased. The size of the sintering neck increased. Figure 4 compares the XRD patterns of the specimens with 30% fly ash and 50% fly ash. It was determined from Fig. 4 that the mineral phases of the specimens changed with increasing amount of fly ash. When the fly ash content increased from 30% to 50%, the main mineral phases of the specimens changed from gehlenite, kirschsteinite, merwinite, and small amounts of magnesium iron oxide and C_2S to gehlenite, kirschsteinite, and a small amount of magnesium iron oxide. It was found by comparing Fig. 1 with Fig. 4 that the main mineral phases of C_3S, C_2S, C_2F, etc. in the steel slag participated in the sintering reaction at high temperatures, and their diffraction peaks disappeared, whereas the diffraction peak of magnesium iron oxide decreased significantly. As the amount of fly ash increased, the ratio of calcium to silicon increased and the diffraction peaks of gehlenite and kirschsteinite were enhanced. These results accorded with the results reported in Ref. [31]. Therefore, by increasing the amount of fly ash in order to increase the ratio of silicon to calcium, the sintering properties of the base material were improved and the densification degree of the specimen was enhanced. The density of the specimen increased and the apparent porosity decreased. The compressive strength of the specimen was enhanced accordingly.

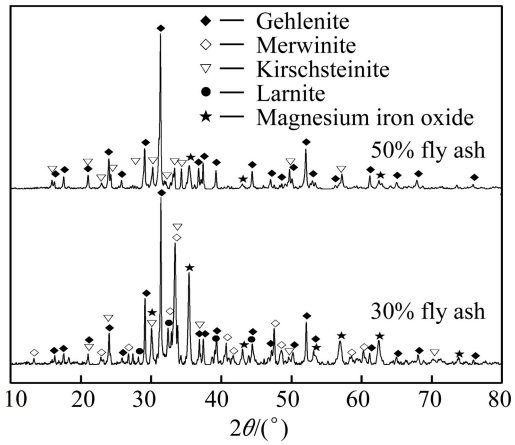

Fig. 4 XRD patterns of specimens with different fly ash contents

Figure 5 shows the test results of the sound-absorption properties of specimens with different fly ash contents. The sound-absorption coefficients of the specimens in the low-frequency range changed

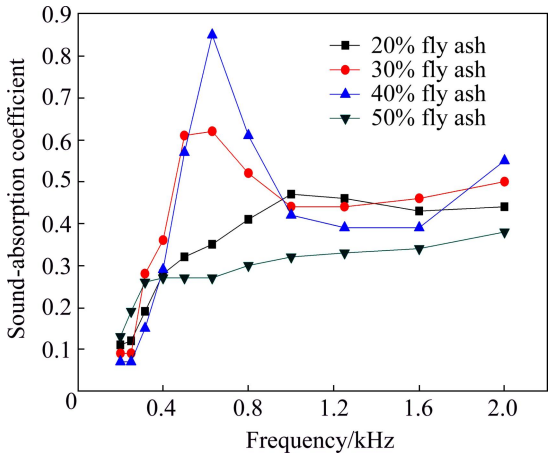

Fig. 5 Effect of fly ash content on sound-absorption properties of specimens

significantly and were between 0.05 and 0.85, whereas the sound-absorption coefficients in the high-frequency range were between 0.30 and 0.55. The sound-absorption performance thus initially increased and then decreased with the increase in the amount of fly ash. The noise reduction coefficient (NRC) was between 0.29 and 0.41. The sintering reaction of the porous materials was accelerated with increasing fly ash content in the base material. The density, apparent porosity, and pore size of the porous sound-absorbing material changed. The apparent porosity did not determine the sound-absorption performance of the specimens from the variation of porosity with fly ash addition here; but the aperture in particular, which has more obvious influence on the sound-absorption properties of materials, became finer. Some studies [32−35] found that the sound-absorbing performance would be improved with the decrease of the aperture; as the pore diameter reduces further, the ends of the some pores are closed to form the lateral cavities or enclosed pores and result in the gradual decrease of the sound absorption. The decrease of the pore diameter size increases the friction of sound waves passing through the pores, and more sound energy is converted into heat, so the sound absorption shows an increasing trend with adding fly ash. The NRC of the specimen with 40% fly ash reached 0.40. However, the pore size is too small and sound waves are reflected on the material surface instead of diffraction in the pores, which makes the sound absorption performance of the porous material decrease. Therefore, the NRC of the specimen with 50% fly ash decreased to 0.29. The porous sound-absorption material can be as a resonance sound absorption structure. In a certain range, the porosity decreases and pore size correspondingly is reduced; the speed of sound decreases in the pores and the resonance frequency will be reduced, which can effectively improve the sound-absorption performance at

medium and low frequencies. As a result, the sound absorption coefficient of sample in 500−800 Hz range increased significantly when fly ash was added to 30% or 40% [36−38].

3.2 Effect of sintering temperature on microstructure and properties of sound-absorbing material

The effect of the sintering temperature on the structure and properties of the steel slag porous sound-absorbing material was investigated under conditions of sintering time 9.0 h, 50% fly ash, and 3.0 g waste EPS. Table 3 lists the density, porosity, and compressive strength of the specimens at different sintering temperatures. It was apparent from Table 3 that the sintering temperature had a significant impact on the density, apparent porosity, and compressive strength of the specimens. As the sintering temperature increased, the density of the specimens increased from 1.09 g/cm^3 to 1.86 g/cm^3 and the apparent porosity of the specimens decreased by 20.5%. Correspondingly, the compressive strength of the specimens was improved from 0.83 MPa to 5.03 MPa.

As indicated in Fig. 6, the specimen sintered at 1100 °C (Fig. 6(a)) developed porosity; the aperture size was uniform and the pore shape was irregular. The specimen obtained at 1150 °C (Fig. 6(b)) had fewer pores; the pore size was non-uniform and the pore shape was somewhat round. Also, some closed pores were formed. Figures 6(c) and (d) show the micromorphologies of the pores in the specimens. Sintering temperature had a significant impact on the micromorphologies of the specimens under the same sintering conditions. The specimen sintered at low temperature (1100 °C) had an extensive crystal phase with a clear boundary and crystals of different sizes and shapes. Growth trend of the sintering neck was clear. The pores were larger and had better connectivity. At 1150 °C, the boundary of the crystal phase was no longer apparent and a glassy material gradually formed in the sintered specimen. A sintering neck gradually formed and increased in size. The pore size decreased and the trend of closed-pore formation was apparent. The specimen had a relatively high level of densification. Figure 7 shows the XRD patterns of the specimens prepared at

Table 3 Effect of sintering temperature on density, apparent porosity, and compressive strength of specimens

Sintering temperature/°C	Density/ (g·cm^{-3})	Apparent porosity/%	Compressive strength/MPa
950	1.09	50.1	0.83
1000	1.23	46.4	1.91
1050	1.23	46.2	2.87
1100	1.42	43.0	3.62
1150	1.86	29.6	5.03

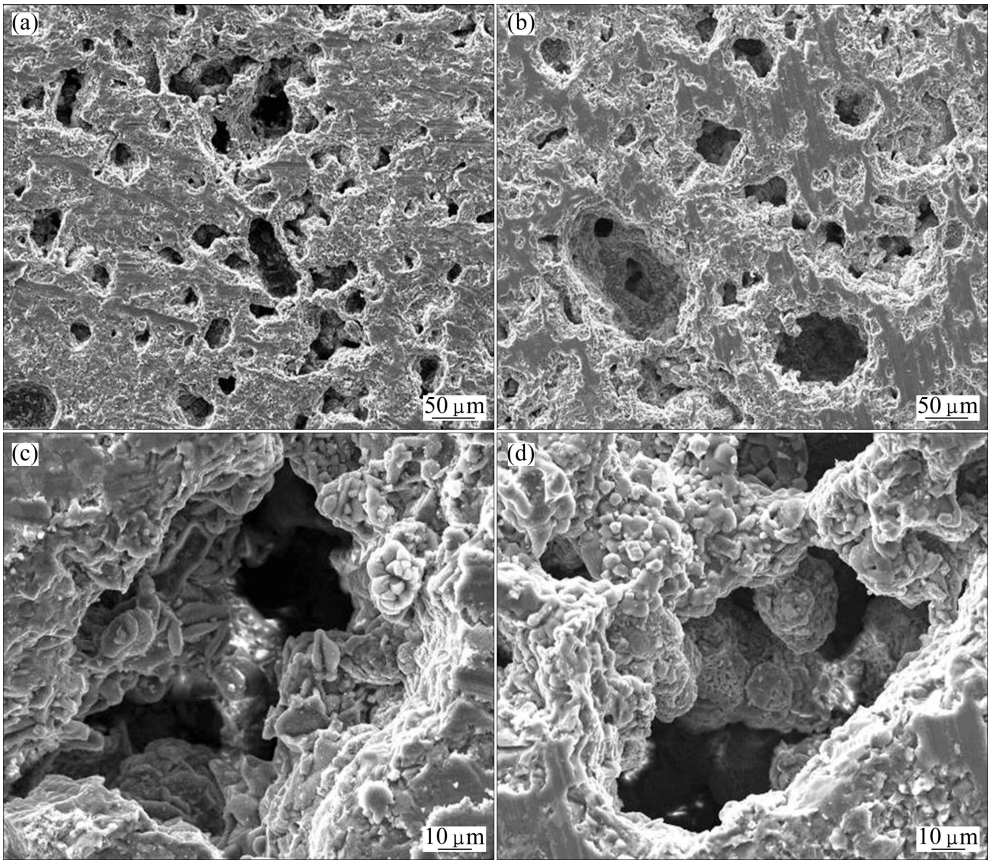

Fig. 6 SEM morphologies and distribution of pores in specimens prepared at different temperatures: (a, c) 1100 °C; (b, d) 1150 °C

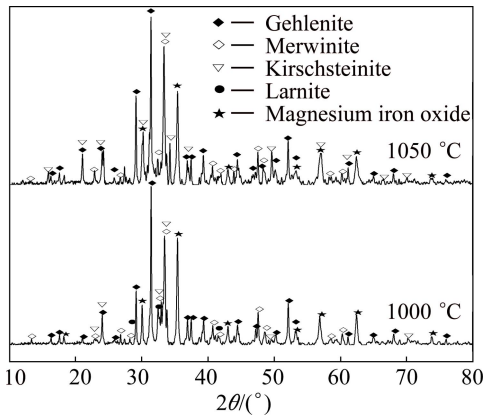

Fig. 7 XRD patterns of specimens prepared at different temperatures

1000 and 1050 °C. The main mineral phases in the specimens sintered at low temperature included gehlenite, kirschsteinite, merwinite, magnesium iron oxide, and a small amount of C_2S. With the increase of sintering temperature, the diffraction peaks of gehlenite and kirschsteinite were enhanced; the diffraction peaks of merwinite and magnesium iron oxide obviously decreased and the diffraction peak of C_2S disappeared. Thus, with increasing sintering temperature, the liquid was added to the system to promote the sintering reaction and the densification of porous sound-absorbing materials was accelerated. The pore shape in the specimen was changed, and some pores were closed or disappeared. The density of the specimens increased continuously with the reduction of the porosity and the compressive strength of the specimens was improved.

Figure 8 shows the sound-absorption coefficients of the specimens prepared at different sintering temperatures. The sound-absorption coefficients of the specimens prepared at different sintering temperatures were between 0.05 and 0.55 at low frequencies and between 0.20 and 0.70 at high frequencies. The sound-absorption performance initially increased and then decreased with increasing sintering temperature. As the sintering temperature increased from 950 °C to 1100 °C, the NRC was improved from 0.13 to 0.42. But the NRC of the specimen prepared at 1150 °C declined to 0.15. With increasing sintering temperature, the density of the porous materials increased and the porosity decreased. As the apparent porosity of specimens changed little before 1100 °C, the sound-absorption performance was mainly affected by pore structure. The pore size was reduced with declining the apparent porosity of specimens, and the sound-absorption performance of the specimens is significantly improved. Many research results of various materials supported this [39−41]. The linear flow resistance increased with the decrease of the pore diameter and air friction increased, which improved the sound-absorption effect [42]. The effect of apparent porosity on the sound-absorption performance became the main factor after 1150 °C. The apparent porosity decreased rapidly, the flow resistance increased to reduce the air permeability, which caused the sound-absorption coefficient of the specimen sintered at 1150 °C to decrease sharply. The specimen sintered at 1100 °C had higher porosity; the pores were more irregular, more uniform and more tortuous, so its sound-absorption coefficient was good and reached 0.42.

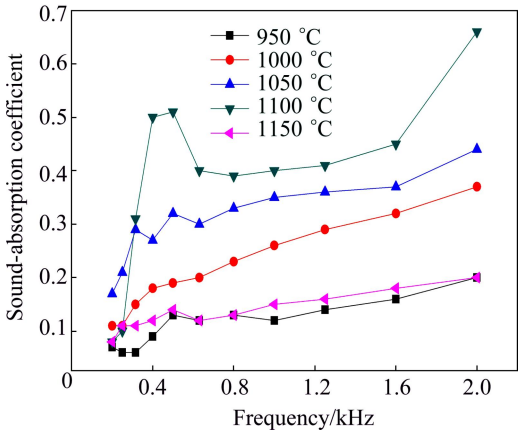

Fig. 8 Effect of sintering temperature on sound-absorption property of specimens

3.3 Effect of sintering time on microstructure and properties of sound-absorbing material

The effect of the sintering time on the structure and properties of the steel slag porous sound-absorbing material was studied under conditions of sintering temperature of 1100 °C, 50% fly ash, and 3.0 g waste EPS. Table 4 shows that as the sintering time increased, the density of the specimens increased from 1.35 g/cm^3 to 1.42 g/cm^3 and the apparent porosity of the specimen decreased by 4.1%. The compressive strength of specimens increased correspondingly from 2.54 MPa to 3.51 MPa. When the sintering time exceeded 7.5 h, the changes of the density, apparent porosity, and compressive strength diminished.

The SEM images shown in Fig. 9 indicate that the specimen sintered for 4.5 h (Fig. 9(a)) had much higher

Table 4 Effect of sintering time on density, apparent porosity, and compressive strength of specimens

Sintering time/h	Density/ (g·cm^{-3})	Apparent porosity/%	Compressive strength/MPa
4.5	1.35	47.2	2.54
6.0	1.36	45.4	2.92
7.5	1.39	44.7	3.27
9.0	1.42	43.1	3.51

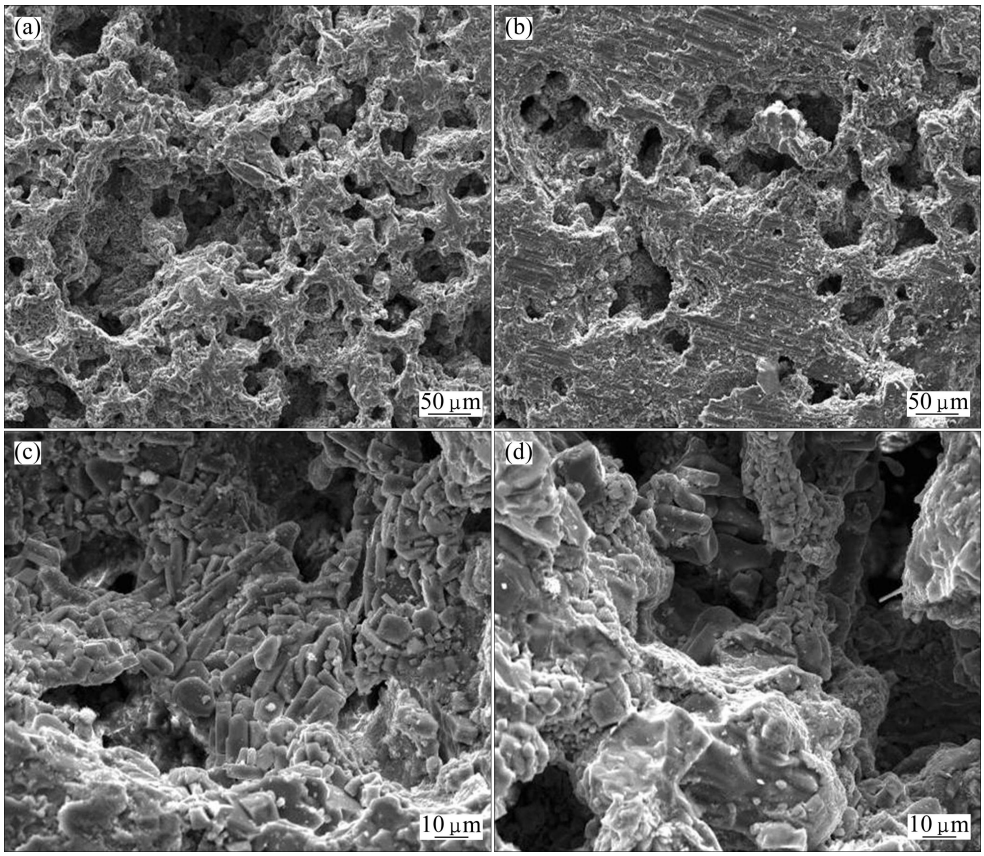

Fig. 9 SEM morphologies and distribution of pores in specimens at different sintering time: (a, c) 4.5 h; (b, d) 9.0 h

porosity than that sintered for 9.0 h (Fig. 9(b)); its pores were larger than those of the specimens sintered for 9.0 h, which were fine, uniform, and had an irregular shape. Figures 9(c) and (d) show that the sintering time impacted the morphology of the specimens to some degree, the specimen with the short sintering time (4.5 h) had many crystal phases with visible crystal boundaries. The phases appeared as stripes and sheets and had different sizes. The pore size was bigger and the size of the sintering neck increased, but the specimen had a low level of densification. The crystal phases grew continuously with increasing sintering time (9.0 h), and the boundaries of some crystal phases diminished. More glassy materials formed. The sintering neck grew continually and the pore size decreased. Figure 10 shows the XRD patterns of the specimens sintered for 4.5 and 9.0 h. The main mineral phases in the specimen sintered for 4.5 h included gehlenite, kirschsteinite, merwinite, a small amount of magnesium iron oxide, and C_2S. With the extension of sintering time, the diffraction peaks of gehlenite and kirschsteinite were enhanced and the diffraction peak of magnesium iron oxide decreased, but the diffraction peak of merwinite and C_2S disappeared. Thus, increasing the sintering time promoted the formation of a mineral phase and completed the sintering reaction. So, the densification of the porous sound-absorbing materials was improved. A few closed pores were formed and the apparent porosity decreased slightly. The density of the specimens also increased and the compressive strength of the specimens was enhanced accordingly.

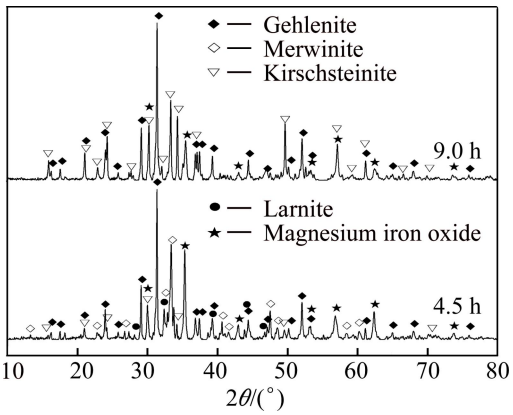

Fig. 10 XRD patterns of specimens at different sintering time

It is shown from Fig. 11 that the sound-absorption coefficients of the specimens are between 0.05 and 0.65 at high frequencies and between 0.40 and 0.60 at low frequencies. The sound-absorption performance was therefore increased with increasing sintering time. The NRC of the specimens sintered for 4.5 and 9.0 h improved from 0.36 to 0.41. The increase of sintering

time had little effect on the density and porosity of the specimens but significantly affected the pore morphology. It is seen from Figs. 9(c) and (d) that the pore size decreased, the pore became more rough and irregular. The main influence factor of sintering time on the sound-absorption performance was similar to that of sintering temperature, and the sound-absorption coefficient of porous materials increased with the decrease aperture. Moreover, irregular pore and rough pore wall also had effect on the sound absorbing performance. The research by YU et al [43] showed that the sound-absorption coefficient of polygonal holes was higher than that of the circular hole at a frequency of 1.6 kHz with the same pore size and thickness of the sample. The specimen after sintering for 7.5 h had irregular, small, and uniform pores with many complicated pore channels. So, its sound-absorption performance was better and its NRC was 0.41.

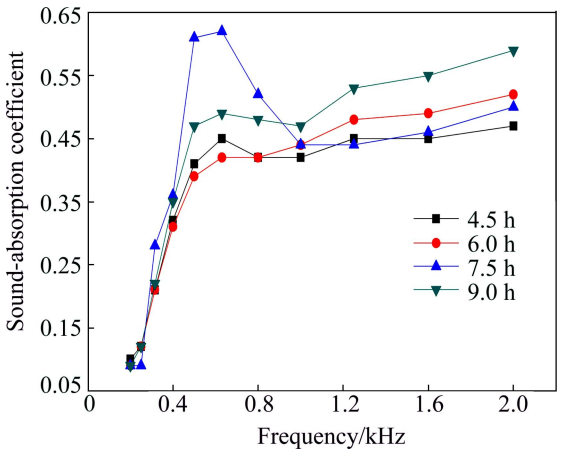

Fig. 11 Effect of sintering time on sound-absorption property of specimens

3.4 Effect of porosity regulation on microstructure and properties of sound-absorbing materials

The influence of the porosity regulation method on the properties of the steel slag porous sound-absorbing material was investigated under conditions of sintering temperature of 1100 °C, sintering time of 7.5 h, and 50% fly ash. Certain generalizations can be derived from the data in Table 5. With the increase in the amount of waste EPS added, the density of the specimen decreased from 1.38 to 1.31 g/cm^3, and the apparent porosity increased by 9.5%; however, the density and porosity did not significantly change when the amount of waste EPS added exceeded 3.6 g. The compressive strength of the specimens decreased from 3.59 to 2.06 MPa.

Table 5 Effect of addition of EPS on density, porosity and compressive strength of specimens

Addition of EPS/g	Density/ (g·cm^{-3})	Apparent porosity/%	Compressive strength/MPa
3.0	1.38	41.8	3.59
3.3	1.37	45.9	3.48
3.6	1.31	50.5	3.10
3.9	1.31	51.3	2.06

The SEM images in Fig. 12 show that the porosity of the specimens obviously increased with increasing amount of waste EPS. The specimen with 3.6 g waste EPS had better developed and better connected pores with non-uniform apertures and irregular shapes. Thus, the addition of EPS significantly improved the porosity and allowed the pores to connect. Although density of the specimen would decrease slightly with the increase of porosity, the compressive strength of the specimen would obviously decrease.

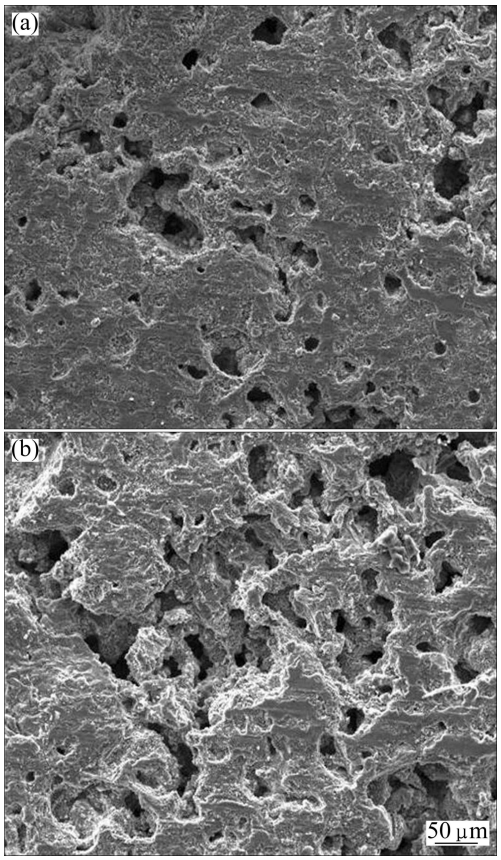

Fig. 12 SEM images showing effect of waste EPS addition on density, porosity, and compressive strength of specimens: (a) 3.0 g EPS; (b) 3.6 g EPS

Figure 13 shows the experimental results of porosity regulation. The sound-absorption properties of the specimens prepared using waste EPS as a pore former at low frequencies were better than those at high frequencies; the sound-absorption coefficients were 0.10−0.85 and 0.35−0.65, respectively. The absorption coefficient was thus improved with increasing amount of waste EPS and the NRC was between 0.40 and 0.48. However, the sound-absorption properties of the

specimens were not obviously improved when the amount of waste EPS exceeded 3.6 g. With increasing waste EPS, the porosity changed very obviously, which had an important influence on the sound-absorption properties of materials. Some previous studies [44,45] reported that it was adverse to improve the sound-absorbing performance that the material had too high or too little porosity; the porosity should have an optimal value. In a certain range, the sound-absorption performance of the sample with high porosity is much better than that of low porosity, and the sound absorption coefficient of the peak moves to the low frequency. Similar study results were obtained in Refs. [46−49]. Increasing the porosity, diffuse reflection or refraction is increased and the vibration of pore wall is enhanced after sound waves enter into the porous material, and the sound waves are attenuated; at the same time, the micro-pores and cracks cause friction and air viscous consumption to increase and the sound absorption performance of the porous materials is improved. Therefore, increasing the amount of waste EPS not only improved the porosity of the specimen, but also enabled the pores to connect and improved the sound-absorption properties of the porous materials at low frequencies, so the NRC could reach about 0.47.

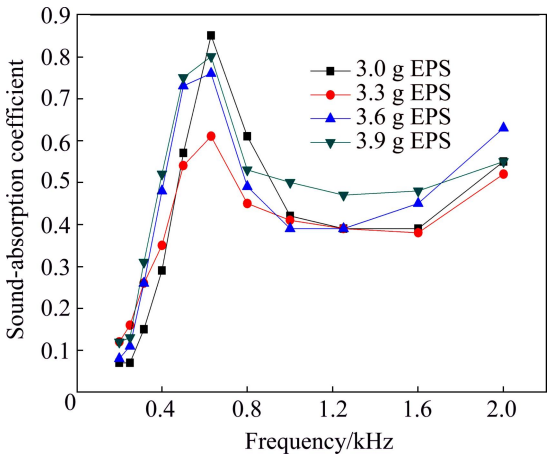

Fig. 13 Effect of addition of EPS on sound-absorption properties of specimens

4 Conclusions

1) Apparent porosity and the NRC of the steel slag porous sound-absorbing material prepared by this method could reach more than 50.0% and 0.47, respectively. The compressive strength of the sintered specimens was above 3.0 MPa.

2) The sound-absorption performance of the materials initially increased and then decreased by increasing fly ash content and sintering temperature, and was improved by extending the sintering time which caused the pore structure of the specimens to change. By adding waste EPS, the apparent porosity and pore connectivity of the specimens were improved, and the sound-absorption performance at low frequencies increased.

3) The optimum preparation conditions for steel slag porous sound-absorbing material were 50% fly ash, 3.6 g waste EPS, sintering temperature 1100 °C, and sintering time 7.5 h, which were determined by analyzing the properties of the sound-absorbing material. The utilization percent of the steel slag could reach higher than 65.0% by this method.

References

[1] GUO Wen-bo, CANG Da-qiang, YANG Zhi-jie, LI Yu, WEI Cheng-zhi. Study on preparation of glass−ceramics from reduced slag after iron melt-reduction [J]. Bulletin of the Chinese Ceramic Society, 2011, 30(5): 1189−1192. (in Chinese)

[2] WANG Yu-ji, YE Gong-xin. A study of mineral phases of oxygen converter slag and their cementious properties [J]. Journal of the Chinese Ceramic Society, 1981, 9(3): 302−308. (in Chinese)

[3] OUYANG Dong, XIE Yu-ping, HE Jun-yuan. Composition, mineral morphology and cementitious properties of converter slag [J]. Journal of the Chinese Ceramic Society, 1991, 19(6): 488−494. (in Chinese)

[4] GEISELER J. Use of steelworks slag in Europe [J]. Waste Management, 1996, 16: 59−63.

[5] ALBAYRAK A T, YASAR M. Investigation of the effects of fatty acids on the compressive strength of the concrete and the grind ability of the cement [J]. Cement and Concrete Research, 2005, 35: 400−404.

[6] XU Guang-liang, QIAN Guang-ren, LAI Zhen-yu, WANG Hai-bin. Study of low-alkalinity steel slag blended oil well cement and geothermal cement—I chemical composition, mineral phases and mineral characteristic of low-alkalinity steel slag [J]. Journal of Southwest University of Science and Technology, 2000, 15(1): 10−14. (in Chinese)

[7] WALIGORA J, BULTEELI D, DEGRUGILLIERS P, DAMIDOT D, POTDEVIN J L, MEASSON M. Chemical and mineralogical characterizations of LD converter steel slags—A multi-analytical techniques approach [J]. Materials Characterization, 2010, 61(1): 39−48.

[8] SHI C J. Steel slag-its production, processing, characteristics, and cementitious properties [J]. Journal of Materials in Civil Engineering, 2004, 16(3): 230−236.

[9] AKIN A, YILMAZ S. Study on steel furnace slags with high MgO as additive in portland cement [J]. Cement and Concrete Research, 2002, 32(8): 1247−1249.

[10] DONG T, TAO Z D, QING C. Study on using steel slag as a raw meal component for cement clinker [C]//Proceedings of 2011 International Conference on Materials for Renewable Energy and Environment. Piscataway: IEEE, 2011: 1193−1196.

[11] FENG C H, LI D X. Effects of steel slag used as iron corrective raw material on the properties of cement clinker [J]. Journal of the Chinese Ceramic Society, 2010, 38(9): 1688−1692.

[12] SHEN W G , ZHOU M K, MA W, HU J Q, CAI Z. Investigation on the application of steel slag–fly ash–phosphogypsum solidified material as road base material [J]. Journal of Hazardous Materials, 2009, 164 (1): 99−104.

[13] POH H Y, GHATAORA G S, GHAZIREH N. Soil stabilization using basic oxygen steel slag fines [J]. Journal of Materials in Civil

Engineering, 2006, 18(2): 229−239.
[14] YANG Jia-kuan, XIAO Bo, TANG Dong-ling, WANG Xiu-ping. Preparation and microstructure analysis of glass-ceramics based on steel slag [J]. Journal of Materials Science & Engineering, 2003, 21(1): 34−36. (in Chinese)
[15] ZHAO Li-hua, CANG Da-qiang, LIU Pu, BAI Hao, TANG Qi. Preparation and microstructure analysis of CaO−MgO−SiO_2 steel-slag ceramics [J]. Journal of University of Science and Technology Beijing, 2011, 33(8): 995−1000. (in Chinese)
[16] YAO Qiang, LU Lei, JIANG Qin, DONG Wei. Preparation and microstructure analysis of glass ceramics based on steel slag [J]. Glass & Enamel, 2005, 33(5): 14−18. (in Chinese)
[17] ZHANG Le-jun, LU Lei, ZHAO Ying. Optimization of the heat-treatment of glass-ceramics prepared from steel slag and fly ash [J]. Materials for Mechanical Engineering, 2008, 32(7): 34−37. (in Chinese)
[18] XIAO Qi-zhong. Expansion and its inhibition of steel slag [J]. Journal of the Chinese Ceramic Society, 1996, 24(6): 635−640. (in Chinese)
[19] XU Guo-tao, WANG Yue, ZHANG Hong-lei. Discussion on the technology of invariability treatment for steel slag [J]. Research on Iron & Steel, 2009, 37(2): 54−56. (in Chinese)
[20] NGUYEN V H, NGO T A T, PHAM H H, NGUYEN N P . Nickel composite plating with fly ash as inert particle [J]. Transactions of Nonferrous Metals Socies of China, 2013, 23(8): 2348−2353.
[21] WANG En, NI Wen, SUN Han. The principle and development of the technique for preparing industrial slags-based geopolymer [J]. Multipurpose Utilization of Mineral Resources, 2005(2): 30−34. (in Chinese)
[22] WANG Ruo-chao, ZHAI Yu-chun, NING Zhi-qiang, MA Pei-hua. Kinetics of SiO_2 leaching from $A1_2O_3$ extracted slag of fly ash with sodium hydroxide solution [J]. Transactions of Nonferrous Metals Society of China, 2014, 24(6): 1928−1936.
[23] MA Da-you. Engineering handbook of noise and vibration control [M]. Beijing: China Machine Press, 2002: 403−413. (in Chinese)
[24] HE Qi-huan. Environmental noise control engineering [M]. Beijing: Tsinghua University Press, 2011: 113. (in Chinese)
[25] DUAN Cui-yun, CUI Guang, XU Xin-bang, LIU Pei-sheng. Sound absorption characteristics of a high-temperature sintering porous [J]. Applied Acoustics, 2012, 73: 865−871.
[26] HE Rui-fei, GUO Zhan-cheng, LI Zhao-jun. Study on making of sound-absorbing porous material using water-granulated slag of blast furnace [J]. Chinese Journal of Environmental Engineering, 2010, 4(12): 2870−2874. (in Chinese)
[27] ZHANG Ji-xiang, LIU Wei, DONG Ying-ge, YANG Jin-long. Study of preparing porous ceramics sound-absorbing material made from gangue [J]. China Ceramics, 2010, 46(6): 50−51. (in Chinese)
[28] ZHANG Fu-shen, XING Ming-fei, WANG Chuan. A method of preparing fly ash sound-absorption material. Chinese Patent: CN101993252A [P]. 2011−03−30. (in Chinese)
[29] LI Peng, GUO Zhan-cheng, SUN Peng, GUO Mao-sheng. Study on preparation of porous sound absorbing material using steel slag [J]. Chinese Journal of Environmental Engineering, 2014, 8(10): 4409−4414. (in Chinese)
[30] WANG Q, YAN P Y. A discussion on improving hydration activity of steel slag by altering its mineral compositions [J]. Journal of Hazardous Materials, 2011, 186: 1070−1075.
[31] ZHAO Hai-jin, YU Qi-jun, WEI Jiang-xiong, GONG Chen-chen, LI Jian-xin, ZHONG Gen. Study on improvement of steel slag property with fly ash added at high temperature [J]. Bulletin of the Chinese Ceramic Society, 2010, 29(3): 572−576. (in Chinese)
[32] LUO Xiang-yu, LI Wen-fang, JIN Xue-li, ZENG Ling-ke. Effects of porosity and pore size on sound absorption characteristic of ceramsite porous material [J]. Journal of the Chinese Ceramic Society, 2011, 39(1): 158−163.
[33] IWASE T. Acoustic properties of porous pavement with double layers and its reduction effects for road traffic noise [C]//Proceedings of Inter Noise. Reston: INVE, 2000: 6−12.
[34] ZHU Bo-quan, FANG Bin-xiang, LI Xiang-cheng, JIANG Xiao. Fractal characteristics of pore structure of corundum based castables [J]. Journal of the Chinese Ceramic Society, 2010, 38(4): 730−734. (in Chinese)
[35] BRENNAN M J, TO W M. Acoustic properties of rigid frame porous materials—An engineering perspective [J]. Applied Acoustics 1998, 62: 793−811.
[36] TANG Hui-ping, ZHU Ji-lei, WANG Jian-yong, GE Yuan, LI Cheng, DI Xiao-bo. Sound absorbing properties of stainless steel fiber porous materials [J]. The Chinese Journal of Nonferrous Metals, 2007, 17(12): 1943−1947. (in Chinese)
[37] HUANG Xue-hui, TANG Hui, TAO Zhi-nan, CHEN Hao. Developments of efficient sound absorption of fiber-gypsum functional composite materials [J]. Journal of Functional Materials, 2007, 38(5): 822−824. (in Chinese)
[38] JIANG Hong-yuan, WU Guo-qi, XIA Yu-hong, ИЗЖЕУРОВЕ А. Experimental research on relationship between metal rubber characteristic parameter and its sound absorption performance [J]. Journal of Vibration and Shock, 2007, 26(11): 54−58. (in Chinese)
[39] HUANG Xue-hui TANG Hui, TAO Zhi-nan. Developments of sound absorption of fine performance polyurethane-based porous composite materials [J]. Materials Review, 2007, 21(6): 152−154. (in Chinese)
[40] ZHOU Dong-liang, ZHANG Zhi-qiang, LI Fu-gang, PAN Zhi-hua, ZHU She-min, JIN Jiang. Preparation of cement based on composite porous sound-absorbing material and its properties [J]. Noise and Vibration Control, 2008, 28(4): 136−140. (in Chinese)
[41] CHENG Gui-ping, CHEN Hong-deng, HE De-ping, SHU Guang-ji, XIAO Jin-xin. Acoustic property of porous aluminum [J]. Journal of Southeast University: Natural Science Edition, 1998, 28(6): 169−172. (in Chinese)
[42] CHANG Bao-jun, WANG Xiao-lin, PENG Feng, SUN Yan. Prediction on the sound absorption performance of fibrous porous metals at high sound pressure levels [J]. Technical Acoustics, 2009, 28(4): 450−453. (in Chinese)
[43] YU Huan, FANG Li-gao, YAN Qing-song. The fabrication of porous aluminum alloys and the testing of the sound absorbent property [J]. Journal of Nanchang University: Engineering & Technology, 2000, 22(4): 10−13. (in Chinese)
[44] CHENG Gui-ping, CHEN Hong-deng, HE De-ping, SHU Guang-ji. Effect of pore structure on acoustic properties of porous aluminum [J]. Materials for Mechanical Engineering, 1999, 23(5): 30−31. (in Chinese)
[45] AO Qing-bo, TANG Hui-ping, ZHU Ji-lei, WANG Jian-yong, ZHI Hao. Sound absorption characteristics of FeCrAl sintering fibrous porous materials [J]. Rare Metal Materials and Engineering, 2009, 38 (10): 1765−1768. (in Chinese)
[46] YU Hai-jun, YAO Guang-chun, WANG Xiao-lin, LI Bing, YIN Yao. Research on sound absorption property of Al−Si closed-cell aluminum foam [J]. Journal of Functional Materials, 2006, 37(12): 2014−2018. (in Chinese)
[47] XU Qing-yan, CHEN Yu-yong, LI Qing-chun. Study on sound absorbent property of porous aluminum alloy [J]. Aerospace Materials & Technology, 1998(2): 39−43. (in Chinese)
[48] WANG Yue. Sound absorption characteristics of foamed aluminum [J]. Development and Application of Materials, 1999, 14(4): 15−18. (in Chinese)
[49] XIE Zhen-kai, IKEDA T, KUDA Y, NAKAJIMA H. Sound absorption characteristics of lotus-type porous copper fabricated by unidirectional solidification [J]. Materials Science and Engineering A, 2004, 386(2): 390−395.

利用钢渣烧结制备多孔吸声材料

孙 朋，郭占成

北京科技大学 钢铁冶金新技术国家重点实验室，北京 100083

摘 要：以废聚苯乙烯颗粒为造孔剂制备钢渣多孔吸声材料，研究粉煤灰添加量、烧结温度、烧结时间和造孔剂掺加量对钢渣多孔材料性能的影响。实验结果显示，该方法制备的多孔吸声材料的显气孔率达到 50.0%以上；材料抗压强度和平均吸声系数分别达到 3.0 MPa 和 0.47 以上。综合考虑材料性能、能源消耗和生产成本，较优的制备条件如下：粉煤灰添加量 50%、废聚苯乙烯颗粒质量 3.6 g、烧结温度 1100 °C 和烧结时间 7.5 h。

关键词：钢渣；多孔吸声材料；降噪系数；孔隙率；抗压强度

(Edited by Wei-ping CHEN)